

Influence of Rashba spin–orbit coupling on Josephson effect in triplet superconductor/two-dimensional semiconductor/triplet superconductor junctions

Bin-Hao Du(杜彬豪), Man-Ni Chen(陈嫚妮), and Liang-Bin Hu(胡梁宾)†

Citation: Chin. Phys. B, 2022, 31 (7): 077201 DOI: 10.1088/1674-1056/ /ac587e
Journal homepage: http://cpb.iphy.ac.cn; http://iopscience.iop.org/cpb

What follows is a list of articles you may be interested in

Understanding of impact of carbon doping on background carrier conduction in GaN

Zhenxing Liu(刘振兴), Liuan Li(李柳暗), Jinwei Zhang(张津玮), Qianshu Wu(吴千树), Yapeng Wang(王亚朋), Qiuling Qiu(丘秋凌), Zhisheng Wu(吴志盛), and Yang Liu(刘扬)
Chin. Phys. B, 2021, 30 (**10**): 107201. DOI: 10.1088/1674-1056/abfa0d

Group velocity matters for accurate prediction of phonon-limited carrier mobility

Qiao-Lin Yang(杨巧林), Hui-Xiong Deng(邓惠雄), Su-Huai Wei(魏苏淮), and Jun-Wei Luo(骆军委)
Chin. Phys. B, 2021, 30 (**8**): 087201. DOI: 10.1088/1674-1056/ac0133

Effects of interface bound states on the shot noise in normal metal-low-dimensional Rashba semiconductor tunnel junctions with induced s-wave pairing potential

Wen-Xiang Chen(陈文祥), Rui-Qiang Wang(王瑞强), Liang-Bin Hu(胡梁宾)
Chin. Phys. B, 2019, 28 (**5**): 057201. DOI: 10.1088/1674-1056/28/5/057201

Influence of spin-orbit coupling on spin-polarized electronic transport in magnetic semiconductor nanowires with nanosized sharp domain walls

Lian Liu(刘恋), Wen-Xiang Chen(陈文祥), Rui-Qiang Wang(王瑞强), Liang-Bin Hu(胡梁宾)
Chin. Phys. B, 2018, 27 (**4**): 047201. DOI: 10.1088/1674-1056/27/4/047201

Unified semiclassical approach to electronic transport from diffusive to ballistic regimes

Hao Geng(耿浩), Wei-Yin Deng(邓伟胤), Yue-Jiao Ren(任月皎), Li Sheng(盛利), Ding-Yu Xing(邢定钰)
Chin. Phys. B, 2016, 25 (**9**): 097201. DOI: 10.1088/1674-1056/25/9/097201

Influence of Rashba spin–orbit coupling on Josephson effect in triplet superconductor/two-dimensional semiconductor/triplet superconductor junctions

Bin-Hao Du(杜彬豪), Man-Ni Chen(陈嫚妮), and Liang-Bin Hu(胡梁宾)†

Guangdong Provincial Key Laboratory of Quantum Engineering and Quantum Materials, School of Physics and Telecommunication Engineering, South China Normal University, Guangzhou 510631, *China*

(Received 11 October 2021; revised manuscript received 12 January 2022; accepted manuscript online 25 February 2022)

We study theoretically Josephson effect in a planar ballistic junction between two triplet superconductors with *p*-wave orbital symmetries and separated by a two-dimensional (2D) semiconductor channel with strong Rashba spin–orbit coupling. In triplet superconductors, three types of orbital symmetries are considered. We use Bogoliubov–de Gennes formalism to describe quasiparticle propagations through the junction and the supercurrents are calculated in terms of Andreev reflection coefficients. The features of the variation of the supercurrents with the change of the strength of Rashba spin–orbit coupling are investigated in some detail. It is found that for the three types of orbital symmetries considered, both the magnitudes of supercurrent and the current-phase relations can be manipulated effectively by tuning the strength of Rashba spin–orbit coupling. The interplay of Rashba spin–orbit coupling and Zeeman magnetic field on supercurrent is also investigated in some detail.

Keywords: Josephson effect, Rashba spin–orbit coupling, triplet superconductor, 0-π transitions

PACS: 72.10.Bg, 72.25.Dc, 72.25.Ba, 72.15.–v **DOI:** 10.1088/1674-1056/ac587e

1. Introduction

In recent years, the study of various effects related to spin–orbit interaction (SOI) of conducting electrons in solid-state materials and their hybrid structures has been an active research field in condensed matter physics. Such studies are not only of fundamental interest but also of practical importance because they may provide some potential routes for spin-based electronics (spintronics) and quantum computation.[1,2] And in this context, strong SOI intrinsic in some narrow-gap semiconductors or topological insulators and various effects related to them have attracted considerable interest. The strong SOI intrinsic in such materials may originate from bulk inversion asymmetry[3] or structural inversion asymmetry due to confining potentials[4] and can be externally controlled by the application of electric field, gate voltage, or mechanical strain, *etc.*, for instance.[5–7] Such tunability has a great potential for the application to spintronic devices and quantum information processing. A variety of interesting phenomena were predicted based on such strong SOI, to name a few, spin Hall effect[8–11] and quantum spin Hall effect,[12,13] topological insulators,[14] topological superconductivity,[15] *etc.*

An interesting subject within these studies is that what influences strong SOI may have on Josephson supercurrent when two superconductors having a phase difference ϕ is connected by a semiconductor channel with strong SOI. This issue has been investigated recently for a variety of junctions containing various semiconductor nanostructures with strong SOI, such as quantum dots,[16–19] carbon nanotubes,[20,21] semiconductor nanowires,[22–25] 2D electron gas,[26] and others.[27] The possibility to control various parameters of the nanostructures allows one to explore different influences of strong SOI on Josephson effect in such devices. It was predicted that Josephson supercurrents through such nanostructures may exhibit a number of novel features. For instance, in some nanostructures the coexistence of strong SOI and Zeeman effect can induce a supercurrent at $\phi = 0$, the so-called anomalous Josephson current.[25–32] From a generic point of view, such novel features arise from the specific spin structure on the Fermi surfaces due to the spin–orbit coupling, which plays an important role in connection with Josephson effect.

In this work we investigate theoretically Josephson effect in planar ballistic junctions consisting of two triplet superconductors (TSCs) with *p*-wave orbital symmetries and connected by a 2D semiconductor channel with strong Rashba SOI. While there has been a growing interest in understanding coherent transport phenomena in Josephson junctions with strong SOI, most of previous studies were focused on hybrid heterostructures involving conventional superconductors with spin-singlet pairing and *s*-wave orbital symmetry. From theoretical points of view, since the pairing potentials are momentum-dependent and change sign on the Fermi surface and the Cooper pairs take the forms of spin-triplet pairing in TSCs, different behaviors would be anticipated compared to the singlet cases.[33,34] For example, due to the intimate relationship between spin-triplet pairing and ferromagnetism, one

†Corresponding author. E-mail: lbhu26@126.com

© 2022 Chinese Physical Society and IOP Publishing Ltd

would anticipate that the effect of strong Rashba SOI, which behaves as a momentum-dependent effective magnetic field, may have sensitive dependence on the orientation of Rashba effective field relative to the TSC vector order parameter, a key parameter of such systems.[35] Moreover, in such systems zero-energy bound states may form at interfaces in a junction, which may also affect significantly the transport properties of a junction.[36] In view of these facts, a deeper understanding of the effect of strong SOI and its interplay with Zeeman magnetic field upon Josephson supercurrents in such systems is desirable. In the current study, we focus on the coherent transport in connection with Josephson supercurrents in planar ballistic junctions consisting of two triplet superconductor leads with p-wave orbital symmetries and connected by a 2D semiconductor channel with strong Rashba SOI. Using the Bogoliubov–de Gennes (BdG) formalism, we investigate systematically the effect of strong Rashba SOI and its interplay with Zeeman effect upon coherent transport in connection with Josephson supercurrents in such junctions.

The paper is organized as follows. In Section 2 we illustrate the theoretical model and the solution of the scattering problem used for the calculations of Josephson supercurrents. In Section 3 we present the numerical results for Josephson supercurrents and current-phase relations obtained by use of the formalism illustrated in Section 2. The features of the variations of supercurrents and current-phase relations with the changes of relevant physical parameters are investigated in some detail. A summary is given in Section 4.

2. Model and formulation

The system under current study is a planar ballistic junction consisting of two identical p-wave superconductors connected by a 2D semiconductor channel with strong Rashba SOI. The junction is grown along the z direction and lies in the y–z plane. The two interfaces between the two superconductor leads and the semiconductor channel are located at $z = 0$ and $z = L$, respectively, and extend along the y direction. An out-of-plane Zeeman magnetic field is applied along the x direction in the semiconductor channel. The BdG equation for quasiparticle (QP) states in the system is given by

$$\begin{bmatrix} \hat{H}_0(\boldsymbol{k}) & \hat{\Delta}(\boldsymbol{k}) \\ \Delta^+(\boldsymbol{k}) & -H_0^*(-\boldsymbol{k}) \end{bmatrix} \Psi(\boldsymbol{k}) = E\Psi(\boldsymbol{k}), \tag{1}$$

where $\hat{H}_0(\boldsymbol{k})$ is the single-electron Hamiltonian, $\hat{\Delta}(\boldsymbol{k})$ is the gap matrix, $\Psi(\boldsymbol{k})$ is the four-component spinor function defined by $\Psi = \left[\psi_\uparrow, \psi_\downarrow, \psi_\uparrow^\dagger, \psi_\downarrow^\dagger\right]^{\mathrm{T}}$. The single-electron Hamiltonian $\hat{H}_0(\boldsymbol{k})$ is

$$\hat{H}_0(\boldsymbol{k}) = \left[\frac{\hbar^2\boldsymbol{k}^2}{2m} - \mu\right]\sigma_0 + \Theta(z)\Theta(L-z)[V_x\sigma_x + \alpha_{\mathrm{R}}(k_z\sigma_y - k_y\sigma_z)], \tag{2}$$

where $\boldsymbol{k} = (k_y, k_z)$ is the 2D wave vector, σ_0 is the 2×2 identity matrix, and $\sigma = (\sigma_x, \sigma_y, \sigma_z)$ the Pauli matrices, $\Theta(z)$ is the step function, α_{R} is the strength of Rashba SOI in the semiconductor channel, $V_x = g\mu_{\mathrm{B}}B$ is the Zeeman energy, with B the magnitude of the Zeeman field and g the Lande factor and μ_{B} the Bohr magneton. For simplicity, we assume equal effective mass m and chemical potential μ in all regions of the junction.

We assume the TSCs to be in an equal-spin-pairing unitary state. For such pairing states, the gap matrix $\hat{\Delta}$ is related to the $\boldsymbol{d}$ vector of the TSCs by $\hat{\Delta} = \mathrm{i}\Delta(\boldsymbol{d}\cdot\boldsymbol{\sigma})\sigma_y$, then the gap matrix for the system under study takes the following form,

$$\begin{aligned}\hat{\Delta}(\boldsymbol{k}) &= \mathrm{i}\Delta_{\mathrm{L}}(\boldsymbol{k})(\boldsymbol{d}_{\mathrm{L}}\cdot\boldsymbol{\sigma})\sigma_y\Theta(-z) \\ &\quad +\mathrm{i}\Delta_{\mathrm{R}}(\boldsymbol{k})(\boldsymbol{d}_{\mathrm{R}}\cdot\boldsymbol{\sigma})\sigma_y\Theta(z-L),\end{aligned} \tag{3}$$

where $\boldsymbol{d}_{\mathrm{L,R}}$ denote the $\boldsymbol{d}$ vectors in the left (L) and right (R) superconductor leads and $\Delta_{\mathrm{L,R}}(\boldsymbol{k})$ the superconducting order parameters, respectively. In particular, we assume that the $\boldsymbol{d}$ vectors $\boldsymbol{d}_{\mathrm{L,R}}$ lie in the x–y plane and their orientations are defined two angles a_{L} and a_{R}, respectively, where $a_{\mathrm{L,R}}$ is the angle between the x axis and $\boldsymbol{d}_{\mathrm{L,R}}$. The explicit forms of $\boldsymbol{d}_{\mathrm{L,R}}$ are then given by

$$\boldsymbol{d}_{\mathrm{L}} = (\cos a_{\mathrm{L}}, \sin a_{\mathrm{L}}, 0), \tag{4}$$

$$\boldsymbol{d}_{\mathrm{R}} = (\cos a_{\mathrm{R}}, \sin a_{\mathrm{R}}, 0). \tag{5}$$

The Josephson supercurrent is related to a difference in the overall phases of the superconducting order parameters in the left and right leads of the junction. We assume that the two superconductor leads differ only in a overall phase of the order parameter, with

$$\Delta_{\mathrm{L}}(\boldsymbol{k}) = \Delta(\boldsymbol{k}) \tag{6}$$

$$\Delta_{\mathrm{R}}(\boldsymbol{k}) = \Delta(\boldsymbol{k})\mathrm{e}^{\mathrm{i}\phi}, \tag{7}$$

in which $\Delta(\boldsymbol{k})$ denotes the orbital pairing states and ϕ the overall phase difference of the superconducting order parameters. We will consider three types of orbital-pairing states, with

$$\Delta(\boldsymbol{k}) = \begin{cases} \Delta(T)k_y/k_F, & p_y\text{-wave}, \\ \Delta(T)k_z/k_F, & p_z\text{-wave}, \\ \Delta(T)(k_z + \mathrm{i}k_y)/k_F, & p_z + \mathrm{i}p_y\text{-wave}, \end{cases} \tag{8}$$

where k_{F} is the Fermi wave vector of the normal state and $\Delta(T) \cong \Delta_0\sqrt{(T_{\mathrm{c}} - T)/T_{\mathrm{c}}}$ ($T_{\mathrm{c}} = \Delta_0/(1.76k_{\mathrm{B}})$) is the weak-coupling temperature-dependent gap magnitude.

We first solve the BdG equations separately in different regions of the junction to obtain the eigenfunctions of quasiparticles (QPs). For dc Josephson effect, only low-energy excitations (with $\mu \gg E$, $|\Delta(\boldsymbol{k})|$) are involved. Under this assumption, the wave vectors can be regarded as approximately equal in magnitude for electron-like and hole-like QPs in the

superconducting regions, *i.e.*, $k_{\rm e} \approx k_{\rm h} \approx k_{\rm F}$, the so-called Andreev approximation. For convenience, in the following we will use a superscript L (R) in the eigenfunctions to denotes QPs in the left lead ($z < 0$) or in the right lead ($z > {\rm L}$) of the junction and use a subscripts r (l) to denote right-going (left-going) QPs. Defining $\boldsymbol{k} \equiv (k_z, k_y) = (k_{\rm F}\cos\theta, k_{\rm F}\sin\theta)$ and $-\hat{\boldsymbol{k}} \equiv (-k_z, k_y)$, where θ is the angle of the wave vector $\boldsymbol{k}$ of a QP relative to the z direction, the eigenfunctions of right-going (left-going) QPs in the left lead ($z < 0$) or in the right lead ($z > {\rm L}$) of the junction can be given by

$$\begin{aligned}
\psi^{\rm L(R)}_{\rm r,e,\uparrow} &= {\rm e}^{{\rm i}k_y y + {\rm i}k_z z}(-u_1 s_1 e_1, 0, v_1, 0)^{\rm T}, \\
\psi^{\rm L(R)}_{\rm r,e,\downarrow} &= {\rm e}^{{\rm i}k_y y + {\rm i}k_z z}(0, u_1 s_1 e_2, 0, v_1)^{\rm T}, \qquad (9)\\
\psi^{\rm L(R)}_{\rm r,h,\uparrow} &= {\rm e}^{{\rm i}k_y y - {\rm i}k_z z}(-v_2 s_2 e_1, 0, u_2, 0)^{\rm T}, \\
\psi^{\rm L(R)}_{\rm r,h,\downarrow} &= {\rm e}^{{\rm i}k_y y - {\rm i}k_z z}(0, v_2 s_2 e_2, 0, u_2)^{\rm T}, \qquad (10)\\
\psi^{\rm L}_{\rm l,e,\uparrow} &= {\rm e}^{{\rm i}k_y y - {\rm i}k_z z}(-u_2 s_2 e_1, 0, v_2, 0)^{\rm T}, \\
\psi^{\rm L}_{\rm l,e,\downarrow} &= {\rm e}^{{\rm i}k_y y - {\rm i}k_z z}(0, u_2 s_2 e_2, 0, v_2)^{\rm T}, \qquad (11)\\
\psi^{\rm L}_{\rm l,h,\uparrow} &= {\rm e}^{{\rm i}k_y y + {\rm i}k_z z}(-v_1 s_1 e_1, 0, u_1, 0)^{\rm T}, \\
\psi^{\rm L}_{\rm l,h,\downarrow} &= {\rm e}^{{\rm i}k_y y + {\rm i}k_z z}(0, v_1 s_1 e_2, 0, u_1)^{\rm T}, \qquad (12)
\end{aligned}$$

where e (h) denotes the types and $\uparrow$ ($\downarrow$) denotes the spins of QPs, and the factors $u_{1,2}$, $v_{1,2}$, $s_{1,2}$, and $e_{1,2}$ are given by

$$u_1 = \sqrt{\frac{E+H_1}{2E}}, \quad v_1 = \sqrt{\frac{E-H_1}{2E}}, \qquad (13)$$

$$u_2 = \sqrt{\frac{E+H_2}{2E}}, \quad v_2 = \sqrt{\frac{E-H_2}{2E}}, \qquad (14)$$

$$s_1 = \frac{\Delta_{\rm L(R)}(\boldsymbol{k})}{|\Delta_{\rm L(R)}(\boldsymbol{k})|}, \quad s_2 = \frac{\Delta_{\rm L(R)}(-\boldsymbol{k})}{|\Delta_{\rm L(R)}(-\boldsymbol{k})|}, \qquad (15)$$

$$e_1 = \cos a_{\rm L(R)} - {\rm i}\sin a_{\rm L(R)}, \quad e_2 = \cos a_{\rm L(R)} + {\rm i}\sin a_{\rm L(R)}, \qquad (16)$$

in which E is the energy of QP, and H_1 and H_2 are defined by

$$H_1 = \sqrt{E^2 - |\Delta(\boldsymbol{k})|^2}, \quad H_2 = \sqrt{E^2 - |\Delta(-\boldsymbol{k})|^2}. \qquad (17)$$

The corresponding eigenfunctions of right-moving (left-moving) electrons (holes) in the semiconductor channel between the two superconductor leads will be denoted as $\psi_{\rm e(h),r(l),\gamma}$, in which the subscripts γ (= + or −) denote the spin helicity. Since the system is translational invariant along the y direction, the y component of the wave vector is conserved when a QP is transmitted through the interfaces between the superconductor leads and the semiconductor channel. For electrons (holes) with energy E and the y component k_y of the wave vector, the eigenfunctions of right-moving (left-moving) electrons (holes) in the semiconductor channel can then be expressed as

$$\psi_{\rm e,r(l),\gamma} = \frac{1}{C_{\rm e,r(l),\gamma}} {\rm e}^{{\rm i}k_y y + {\rm i}s k_{z,{\rm e},\gamma} z}(u_\uparrow, u_\downarrow, 0, 0)^{\rm T}, \qquad (18)$$

$$\psi_{\rm h,r(l),\gamma} = \frac{1}{C_{\rm h,r(l),\gamma}} {\rm e}^{{\rm i}k_y y - {\rm i}s k_{z,{\rm h},\gamma} z}(0, 0, v_\uparrow, v_\downarrow)^{\rm T}, \qquad (19)$$

where $C_{\rm e,r(l),\gamma}$ is the normalization factor, $s = +$ for right-moving and $s = -$ for left-moving electrons (holes), $k_{z,{\rm e(h)},\gamma}$ denotes the z component of the wave vector of an electron (hole) with the spin helicity γ, and $u_\uparrow$, $u_\downarrow$, $v_\uparrow$, $v_\downarrow$ are defined by

$$\begin{aligned}
u_\uparrow &= -V_x + {\rm i}s\alpha_{\rm R} k_{z,{\rm e},\gamma}, \\
u_\downarrow &= \frac{\hbar^2}{2m}(k^2_{z,{\rm e},\gamma} + k_y^2) - \mu - \alpha_{\rm R} k_y, \qquad (20)\\
v_\uparrow &= V_x + {\rm i}s\alpha_{\rm R} k_{z,{\rm h},\gamma}, \\
v_\downarrow &= -\frac{\hbar^2}{2m}(k^2_{z,{\rm h},\gamma} + k_y^2) + \mu - \alpha_{\rm R} k_y. \qquad (21)
\end{aligned}$$

In Eqs. (18)–(21), the z component of the wave vector of an electron (hole) with the spin helix index γ is given by $k_{z,{\rm e(h)},\gamma} = \sqrt{k^2_{{\rm e(h)},\gamma} - k_y^2}$, where $k_{{\rm e(h)},\gamma}$ is the magnitude of the wave vector of an electron (hole) with the spin helix index γ. The energy dependence of $k_{{\rm e(h)},\gamma}$ is determined by the dispersion relations in the semiconductor channel, which reads

$$E = \frac{\hbar^2 \boldsymbol{k}^2}{2m} - \mu - \gamma\sqrt{V_x^2 + \alpha_{\rm R}^2 \boldsymbol{k}^2} \qquad (22)$$

for electrons, and

$$E = -\frac{\hbar^2 \boldsymbol{k}^2}{2m} + \mu + \gamma\sqrt{V_x^2 + \alpha_{\rm R}^2 \boldsymbol{k}^2} \qquad (23)$$

for holes. For low-energy excitations with $E \ll \mu$, $k_{{\rm e(h)},\gamma}$ can be given by

$$\begin{aligned}
k_{\rm e,+} &\approx k_{\rm h,+} \\
&\approx \sqrt{k_{\rm F}^2 + \frac{2m^2\alpha_{\rm R}^2}{\hbar^4} + \frac{2m}{\hbar^2}\sqrt{V_x^2 + \alpha_{\rm R}^2 k_{\rm F}^2 + \frac{m^2\alpha_{\rm R}^4}{\hbar^4}}}, \qquad (24)\\
k_{\rm e,-} &\approx k_{\rm h,-} \\
&\approx \sqrt{k_{\rm F}^2 + \frac{2m^2\alpha_{\rm R}^2}{\hbar^4} - \frac{2m}{\hbar^2}\sqrt{V_x^2 + \alpha_{\rm R}^2 k_{\rm F}^2 + \frac{m^2\alpha_{\rm R}^4}{\hbar^4}}}. \qquad (25)
\end{aligned}$$

Note that the wave vectors $k_{{\rm e(h)},\gamma}$ depend on both the Rashba SOI strength and the Zeeman energy in the semiconductor channel. This has significant influence on the propagation of electrons and holes in the semiconductor channel. For example, if the Zeeman energy $V_x > \mu$ and $\alpha_{\rm R} = 0$, the wave vectors $k_{{\rm e(h)},-}$ of minority-spin QPs will be imaginary, implying that their propagations will be exponentially suppressed in the semiconductor channel.

Now we consider the scattering problem of QPs through the junction. By use of the eigenfunctions (9)–(12) and (18)–(19), the following wavefunction ansatz can be constructed for a spin-σ electron-like QP injected from the left lead of the junction:

$$\Psi_{\mathrm{e},\sigma}(\boldsymbol{r}) = \Theta(-z)\left\{\psi^{\mathrm{L}}_{\mathrm{r,e},\sigma} + \sum_{\sigma'=\uparrow\downarrow}\left[a^{\mathrm{e}}_{\sigma\sigma'}\psi^{\mathrm{L}}_{\mathrm{l,h},\sigma'} + b^{\mathrm{e}}_{\sigma\sigma'}\psi^{\mathrm{L}}_{\mathrm{l,e},\sigma'}\right]\right\} + \Theta(z)\Theta(L-z)\Big\{c^{\mathrm{e}}_{\sigma+}\psi_{\mathrm{r,e},+} + c^{\mathrm{e}}_{\sigma-}\psi_{\mathrm{r,e},-} + d^{\mathrm{e}}_{\sigma+}\psi_{\mathrm{r,h},+}$$
$$+ d^{\mathrm{e}}_{\sigma-}\psi_{\mathrm{r,h},-} + f^{\mathrm{e}}_{\sigma+}\psi_{\mathrm{l,e},+} + f^{\mathrm{e}}_{\sigma-}\psi_{\mathrm{l,e},-} + w^{\mathrm{e}}_{\sigma+}\psi_{\mathrm{l,h},+} + w^{\mathrm{e}}_{\sigma-}\psi_{\mathrm{l,h},-}\Big\} + \Theta(z-L)\sum_{\sigma'=\uparrow\downarrow}\left[g^{\mathrm{e}}_{\sigma\sigma'}\psi^{R}_{\mathrm{r,e},\sigma'} + h^{\mathrm{e}}_{\sigma\sigma'}\psi^{R}_{\mathrm{r,h},\sigma'}\right], \tag{26}$$

where $a^{\mathrm{e}}_{\sigma\sigma'}$ are the Andreev reflection coefficients, $b^{\mathrm{e}}_{\sigma\sigma'}$ are the normal reflection coefficients, $g^{\mathrm{e}}_{\sigma\sigma'}$ and $h^{\mathrm{e}}_{\sigma\sigma'}$ are the transmission coefficients, and $c^{\mathrm{e}}_{\sigma\gamma}$, $d^{\mathrm{e}}_{\sigma\gamma}$, $f^{\mathrm{e}}_{\sigma\gamma}$, $w^{\mathrm{e}}_{\sigma\gamma}$ ($\gamma = \pm$) are the coefficients describing the propagation of QPs in the semiconductor channel between the two superconductor leads. There are 16 unknown coefficients in total in the wavefunction (26). These coefficients can be determined by the boundary conditions at the interfaces at $z = 0$ and $z = L$, which read

$$\Psi_{\mathrm{e(h)},\sigma}(\boldsymbol{r})\,|_{z=0^-} = \Psi_{\mathrm{e(h)},\sigma}(\boldsymbol{r})\,|_{z=0^+}, \tag{27}$$
$$\Psi_{\mathrm{e(h)},\sigma}(\boldsymbol{r})\,|_{z=L+0^-} = \Psi_{\mathrm{e(h)},\sigma}(\boldsymbol{r})\,|_{z=L+0^+}, \tag{28}$$
$$\hat{v}_z\Psi_{\mathrm{e(h)},\sigma}(\boldsymbol{r})\,|_{z=0^-} = \hat{v}_z\Psi_{\mathrm{e(h)},\sigma}(\boldsymbol{r})\,|_{z=0^+}, \tag{29}$$
$$\hat{v}_z\Psi_{\mathrm{e(h)},\sigma}(\boldsymbol{r})\,|_{z=L+0^-} = \hat{v}_z\Psi_{\mathrm{e(h)},\sigma}(\boldsymbol{r})\,|_{z=L+0^+}, \tag{30}$$

where

$$\hat{v}_z = \frac{1}{\hbar}\frac{\partial \hat{H}_{\mathrm{BdG}}}{\partial k_z}$$

is the velocity operator, with $\hat{H}_{\mathrm{BdG}}$ the BdG Hamiltonian given in Eq. (1). Substituting the wavefunction (26) into the boundary conditions (27)–(30), we can obtain all unknown coefficients in the wavefunction (26) by numerical calculation. Similar wavefunction ansatz can also be constructed for a spin-σ hole-like QP injected from the left lead of the junction, and the coefficients characterizing various reflection and transmission processes will be denoted correspondingly as $a^{\mathrm{h}}_{\sigma\sigma'}$, $b^{\mathrm{h}}_{\sigma\sigma'}$, *etc.* These coefficients can also be determined through the boundary conditions (27)–(30) by numerical calculations.

The Josephson supercurrent flowing through the junction can be obtained by use of the Furusaki–Tsukada formulas.[37–40] This is written in terms of the Andreev reflection coefficients $a^{\mathrm{e}}_{\sigma\sigma'}$ of injected electron-like QPs and the Andreev reflection coefficients $a^{\mathrm{h}}_{\sigma\sigma'}$ of injected hole-like QPs as follows:

$$I = \frac{e}{2\hbar\beta}\int \mathrm{d}k_y \sum_{\omega_n}\sum_{\sigma}\left\{\frac{|\Delta(\boldsymbol{k})|}{\sqrt{\omega_n^2 + |\Delta(\boldsymbol{k})|^2}}a^{\mathrm{e}}_{\sigma\sigma} - \frac{|\Delta(-\boldsymbol{k})|}{\sqrt{\omega_n^2 + |\Delta(-\boldsymbol{k})|^2}}a^{\mathrm{h}}_{\sigma\sigma}\right\}, \tag{31}$$

where the energy argument is analytically continued to Matsubara frequencies $[E \to \mathrm{i}\omega_n = \mathrm{i}(2n+1)\pi/\beta]$ and $\beta = 1/k_{\mathrm{B}}T$.

3. Results and discussion

In this section we present the numerical results obtained by using the formalism outlined above. For convenience, in the numerical calculations we re-scale the strength of Rashba SOI to a dimensionless parameter $\alpha \equiv 2m\alpha_{\mathrm{R}}/\hbar^2 k_{\mathrm{F}}$, and the superconducting pairing potential Δ_0 and the Zeeman energy V_x are both measured in units of the chemical potential μ. The temperature T is measured in units of the critical temperature T_{c} and the length L of the semiconductor channel between two superconductor leads is measured in units of $1/k_{\mathrm{F}}$. The supercurrent is measured in units of $e\Delta_0/\hbar$.

For clarity, we first investigate the effect of Rashba SOI in the absence of Zeeman effect. We calculate numerically the supercurrent as a function of the phase difference ϕ of the superconducting order parameters for several different values of the Rashba SOI strength α and the Zeeman energy $V_x = 0$. The corresponding results for p_y-wave pairing, p_z-wave pairing, and $(p_z + \mathrm{i}p_y)$-wave pairing are plotted in Figs. 1(a)–1(c), respectively. From Figs. 1(a)–1(c) one can see that, in the presence of Rashba SOI, the current-phase relations are still nearly in the ordinary form of a sinusoidal function for the three types of orbital symmetries, as in the absence of Rashba SOI. But the magnitude of supercurrent can be changed significantly in the presence of Rashba SOI and can be tuned effectively by varying the strength of Rashba SOI. More interestingly, from Figs. 1(a)–1(c) one can see that the so-called 0–π transitions can be driven by varying the strength of Rashba SOI, *i.e.*, as the strength of Rashba SOI is varied, the direction of supercurrent is reversed at some critical values of the Rashba SOI strength and the current-phase relation changes from the form of $I(\phi) \propto \sin\phi$ (0-state) to the form of $I(\phi) \propto \sin(\phi + \pi)$ (π-state), or *vice versa*. Such transitions can be more clearly illustrated by analyzing the sign changes of the supercurrent $I(\phi)$ at a fixed phase difference ϕ with the variation of the Rashba SOI strength α. In Figs. 2(a)–2(c) we plot $I(\phi)$ at $\phi = \pi/2$ as a function of the Rashba SOI strength α for p_y-wave and p_z-wave and $(p_z + \mathrm{i}p_y)$-wave pairing, respectively. Figures 2(a)–2(c) show that the magnitudes of the supercurrents at $\phi = \pi/2$ (the critical supercurrents) oscillate in an approximately periodic way with the variation of the Rashba SOI strength α, but the amplitudes of the oscillation decrease gradually with the increase of α. Accompanying with the oscillation of the mag-

nitude of supercurrent, the direction of supercurrent is reversed for several times at some critical values of the parameter α, resulting in a sequence of 0–π transitions. In Fig. 2(a)–2(c), the sequence of alternating 0 and π states is separated by a sequence of critical points of the parameter α at which the supercurrent changes sign, beginning with a 0-state at $\alpha = 0$ for all the three types of pairing symmetries. Since the strength of Rashba SOI can be tuned by electrical means, this result suggests that it is possible to realize 0–π transitions by electrical means. We also note that as the Rashba SOI strength is varied, the magnitude of the supercurrent remains vanishing at $\phi = 0$, *i.e.*, no anomalous Josephson supercurrent is exhibited, unlike the results found in some *s*-wave Josephson junctions with Rashba SOI.[25–32]

From Fig. 2(a)–2(c) one can note that the features of the oscillations of the supercurrents with the variation of the Rashba SOI strength depend on the orbital symmetries of the pairing potentials in the superconducting leads. For example, for the cases of p_y-wave pairing, the amplitude of the oscillation of the supercurrent with the increase of the parameter α decreases rapidly, while for the cases of p_z-wave and $(p_z + \mathrm{i}p_y)$-wave pairing, the amplitude of the oscillation of the supercurrent with the increase of the parameter α decreases more slowly. For the cases of p_y-wave pairing shown in Fig. 2(a), the oscillation of the supercurrent is substantial only in the range of $\alpha < 1$. Outside this range, the oscillation of the supercurrent is much weak and the oscillation almost can not result in 0–π transition as the value of α is increased. In the range of $\alpha > 1.5$, the π-state is much robust to increasing α and no 0–π transitions are observed. In contrast, for the cases of p_z-wave and $(p_z + \mathrm{i}p_y)$-wave pairing shown in Figs. 2(b) and 2(c), the oscillations of the supercurrents with the variation of the parameter α are substantial and can lead to 0–π transitions in a more wide range of the parameter α. For a given value of the parameter α, whether the ground state is a 0-state or a π-state also depends on the orbital symmetries of the pairing potentials in the superconducting leads. For example, for the cases shown in Fig. 2(a)–2(c), the ground state is a 0-state at $\alpha = 0.5$ for p_y-wave pairing but is a π-state for p_z-wave and $(p_z + \mathrm{i}p_y)$-wave pairing.

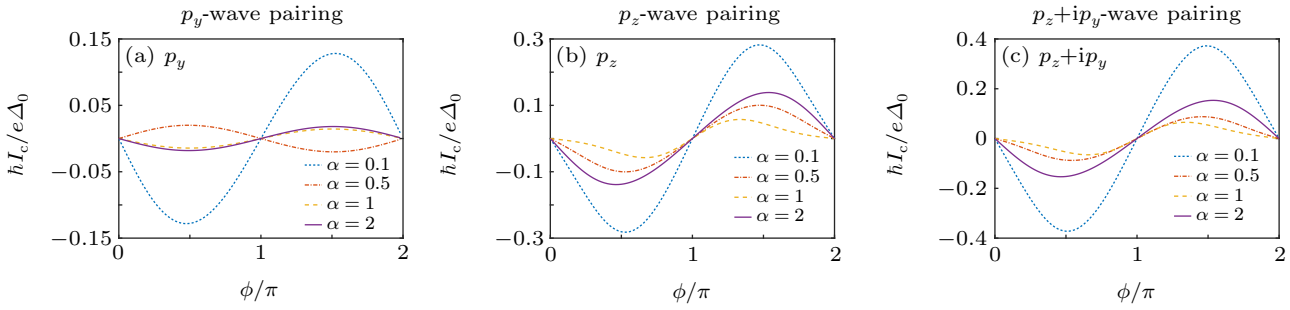


Fig. 1. The supercurrent as a function of the phase difference ϕ of the superconducting order parameters for several different values of the Rashba SOI strength α. The corresponding results for p_y-wave and p_z-wave and $(p_z + \mathrm{i}p_y)$-wave pairings are plotted in panels (a), (b), and (c), respectively. The values of the parameter α are shown in the figures. The other parameters are $\Delta_0/\mu = 0.001$, $V_x = 0$, $T/T_c = 0.4$, $k_F L = 20$, $a_L = a_R = 0$.

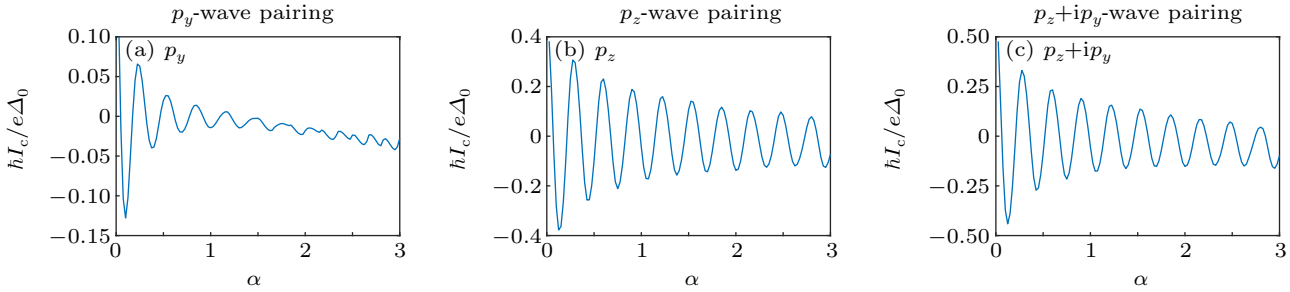


Fig. 2. The supercurrent at the phase difference $\phi = \pi/2$ as a function of the Rashba SOI strength α for (a) p_y-wave pairing, (b) p_z-wave pairing, (c) $(p_z + \mathrm{i}p_y)$-wave pairing, respectively. The parameters are $\Delta_0/\mu = 0.001$, $V_x = 0$, $T/T_c = 0.4$, $k_F L = 20$, $a_L = a_R = 0$.

From the theoretical point of view, for the system considered above, when a QP incident from one superconducting electrode is reflected at the junction interfaces or is transmitted to the other superconducting electrode through the semiconductor channel between them, since the y component of the wave vector is conserved but the z component is not conserved, the strength of the pairing potential experienced by a QP does not change if the orbital symmetry of the pairing potential is p_y-wave type but will be changed if the orbital symmetry is p_z-wave or $(p_z + \mathrm{i}p_y)$-wave type. The phase changes of the wave functions of reflected (or transmitted) QPs will also be different for different orbital symmetries. Due to such differences, the features of the oscillations of the supercurrents with the variation of the Rashba SOI strength depend on the orbital symmetries of the pairing potentials in the superconducting leads, and compared with the cases of p_y-wave pairing, the oscillations of the supercurrents with the variation of the Rashba SOI strength are more substantial in the cases of p_z-wave or

$(p_z + \mathrm{i}p_y)$-wave pairing, as shown in Fig. 2. And from this point of view, one may expect that the p_z-wave or $(p_z + \mathrm{i}p_y)$-wave type of junctions should be the optimal for observing such oscillations in experiments.

The effects of Rashba SOI illustrated in Figs. 1 and 2 are similar to that of an external magnetic field. This is reasonable since Rashba SOI is equivalent to a momentum-dependent Zeeman field in principle. To illustrate this point more clearly, in Figs. 3(a)–3(c) we plot the supercurrent as a function of the phase difference ϕ of the superconducting order parameters for several different values of the Zeeman energy V_x and the Rashba SOI strength $\alpha = 0$ for p_y-wave and p_z-wave and $(p_z + \mathrm{i}p_y)$-wave pairings, respectively, and in Figs. 4(a)–4(c) we plot the corresponding results for the supercurrent at the phase difference $\phi = \pi/2$ as a function of the Zeeman energy V_x. From Figs. 3 and 4 one can see that, in the regime $V_x/\mu < 1$, the supercurrent exhibits significant oscillations with the increase of the Zeeman energy V_x, similar to that as shown in Figs. 1 and 2. In the regime $V_x/\mu > 1$, the supercurrent is suppressed significantly. This suppression is due to the fact that the wave vector $k_{\mathrm{e(h)},-}$ of minority-spin QPs become imaginary when $V_x/\mu > 1$ (as can be seen from Eq. (25)) and their propagations in the semiconductor channel between the two superconductor leads is exponentially suppressed and hence do not contribute to the supercurrent. In the regime $V_x/\mu < 1$, the magnitude of the supercurrent decreases in an oscillatory manner with the increase of the Zeeman energy V_x, and accompanying with the oscillation of the magnitude of the supercurrent, the direction of the supercurrent is also reversed for several times, *i.e.*, the oscillation of the supercurrent with the increase of the Zeeman energy also leads to a sequence of 0–π transitions. In Fig. 4(a)–4(c), such transitions are indicated by the sign changes of the supercurrent at some critical values of V_x, which separate a sequence of alternating 0 and π states, beginning with a 0-state at $V_x = 0$ for all the three types of pairing symmetry.

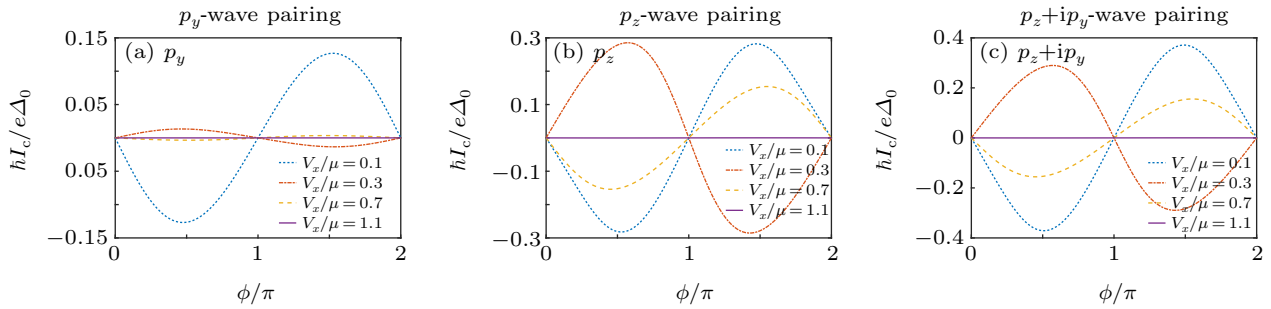


Fig. 3. The supercurrent as a function of the phase difference ϕ of the superconducting order parameters for several different values of the Zeeman energy V_x. The corresponding results for p_y-wave pairing, p_z-wave pairing, and $(p_z + \mathrm{i}p_y)$-wave pairing are plotted in panels (a), (b), and (c), respectively. The values of V_x (in units of μ) are shown in the figures. The other parameters are $\Delta/\mu = 0.001$, $\alpha = 0$, $T/T_c = 0.4$, $k_F L = 20$, $a_L = a_R = 0$.

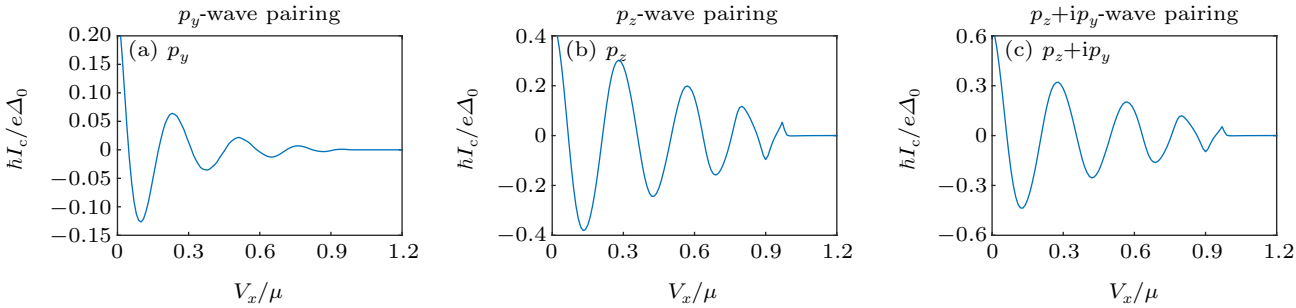


Fig. 4. The supercurrent at the phase difference $\phi = \pi/2$ as a function of the Zeeman energy V_x for (a) p_y-wave pairing, (b) p_z-wave pairing, (c) $(p_z + \mathrm{i}p_y)$-wave pairing, respectively. The parameters are $\Delta_0/\mu = 0.001$, $\alpha = 0$, $T/T_c = 0.4$, $k_F L = 20$, $a_L = a_R = 0$.

If both Rashba SOI and Zeeman magnetic field are present, the supercurrent and current-phase relation will depend both on Rashba SOI and Zeeman magnetic field. In such cases, some features of the supercurrents and current-phase relations illustrated above may be altered significantly if the interplay of Rashba SOI and Zeeman magnetic field is strong. As an example, in Figs. 5(a)–5(c) we plot the supercurrent at the phase difference $\phi = \pi/2$ as a function of the Zeeman energy V_x for several different values of the Rashba SOI strength α. From Figs. 5(a)–5(c) one can see that, in the presence of the interplay of Rashba SOI and Zeeman effect, the 0–π transitions can still be driven by varying the strength of Zeeman magnetic field or varying the strength of Rashba SOI, but the basic patterns of the variations of the supercurrents with the relevant parameters may be altered significantly due to their interplay. For instance, for the cases with $\alpha = 0.1$ in Fig. 5, the variations of the supercurrent with the Zeeman energy V_x are similar to that as shown in Fig. 4. But as the value of α is increased, *e.g.*, for the cases with $\alpha = 1$, the onset of the oscillation of the supercurrent will require a larger V_x and the

oscillation will become smoother and smoother. As the value of α is increased further, the oscillation of the supercurrent may eventually be smeared out (*e.g.*, for the cases with $\alpha = 2$ in Fig. 5). Another interesting result of the interplay of Rashba SOI and Zeeman effect is that, if the value of α is sufficiently large, the supercurrent will not be suppressed completely even when $V_x/\mu > 1$. Such features are different from that illustrated in Fig. 4. From the theoretical point of view, Rashba SOI not only modify the spin structure on the Fermi surfaces and change the Fermi momenta which affect the Josephson supercurrent but also cause precession of the spins of QPs, which tends to wash out the spin polarization of QPs due to Zeeman effect. In strong spin–orbit coupling regime, the Andreev reflection may be influenced significantly by the wash-out of the spin polarization of QPs and hence the suppression of Josephson supercurrent due to Zeeman effect may be weakened even when $V_x/\mu > 1$. This is similar to the result obtained in a recent study,[35] where the interplay of Rashba spin–orbit coupling and Zeeman effect on the tunneling conductance of a 2D Rashba metal/superconductor junction is investigated. It was found that, when the Zeeman energy is larger than the Fermi energy, the zero-bias conductance is suppressed in weak spin–orbit coupling regime but may revive in strong spin–orbit coupling regime.[35]

In all cases considered above we have assumed that the directions of the $\boldsymbol{d}$ vectors in two superconducting leads of a junction are parallel to each other and both $\boldsymbol{d}_{\rm L}$ and $\boldsymbol{d}_{\rm R}$ are along the x axis, with the angles $a_{\rm L} = a_{\rm R} = 0$. From the theoretical point of view, the relative orientations of the $\boldsymbol{d}$ vectors in different superconducting leads of a junction may also have significant influence on coherent transport of QPs in connection with Josephson supercurrent. To illustrate this point, we keep the direction of $\boldsymbol{d}_{\rm L}$ along the x axis and rotate $\boldsymbol{d}_{\rm R}$ in the x–y plane, *i.e.*, keeping the angle $a_{\rm L} = 0$ and varying the values of the angle $a_{\rm R}$. In Fig. 6 we plot the supercurrent as a function of the phase difference ϕ of the superconducting order parameters for $a_{\rm R} = 0$, $\pi/2$, and π, respectively. The other parameters are $\Delta/\mu_{\rm s} = 0.001$, $\alpha = 0.1$, $V_x = 0.1$, $T/T_{\rm c} = 0.4$, $k_{\rm F}L = 20$. For the parameters chosen, the ground state of the junction is a 0-state for $a_{\rm R} = 0$ (the directions of $\boldsymbol{d}_{\rm L}$ and $\boldsymbol{d}_{\rm R}$ are parallel to each other) and is a π-state for $a_{\rm R} = \pi$ (the directions of $\boldsymbol{d}_{\rm L}$ and $\boldsymbol{d}_{\rm R}$ are antiparallel to each other) for all the three types of orbital symmetries considered. For $a_{\rm R} = 0$ and $a_{\rm R} = \pi$, the periodicity of the current-phase relationship is 2π. For $a_{\rm R} = \pi/2$, the periodicity of the current-phase relationship is π but not 2π, indicating that the $\sin\phi$ component of the Josephson supercurrent is suppressed and the $\sin 2\phi$ component is enhanced when the directions of the $\boldsymbol{d}$ vectors in two superconducting leads are perpendicular to each other. Such differences indicate clearly that in p-wave Josephson junctions the relative orientations of the $\boldsymbol{d}$ vectors in different superconducting leads may have significant influence on Josephson supercurrent, and both the magnitude of supercurrent and the current-phase relation may be manipulated effectively by tuning the relative orientations of the $\boldsymbol{d}$ vectors in different superconducting leads. Such features are significantly different from that found in conventional s-wave Josephson junctions.

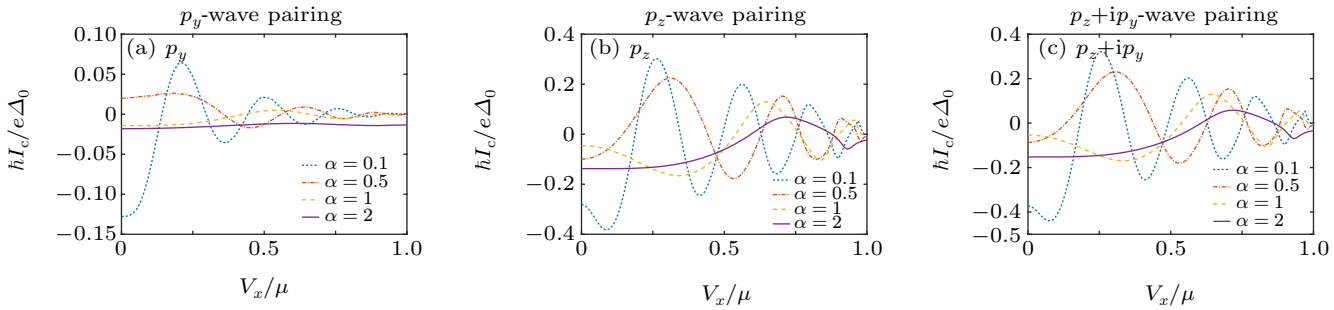


Fig. 5. The supercurrent at the phase difference $\phi = \pi/2$ as a function of the Zeeman energy V_x for several different values of the Rashba SOI strength α. The corresponding results for p_y-wave pairing, p_z-wave pairing, and $(p_z + {\rm i}p_y)$-wave pairing are plotted in panels (a), (b), and (c), respectively. The values of the Rashba SOI strength α are shown in the figures. The other parameters are $\Delta/\mu_{\rm s} = 0.001$, $T/T_{\rm c} = 0.4$, $k_{\rm F}L = 20$, $a_{\rm L} = a_{\rm R} = 0$.

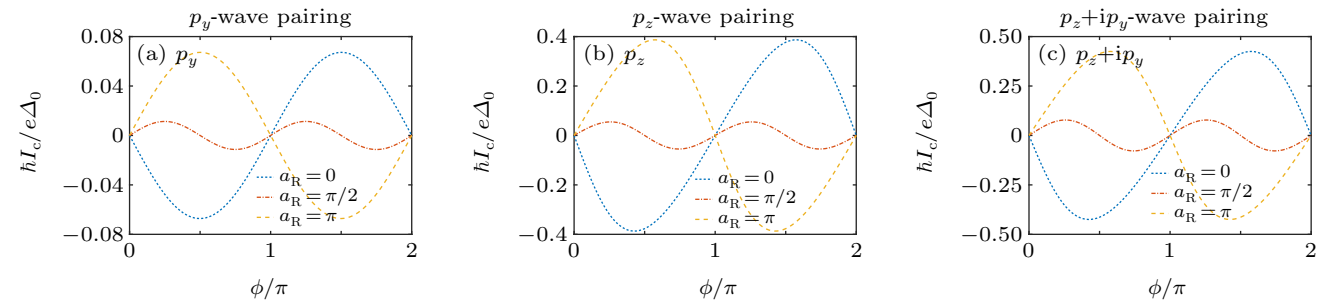


Fig. 6. The supercurrent as a function of the phase difference ϕ of the superconducting order parameters for several different values of the angle $a_{\rm R}$. The corresponding results for p_y-wave pairing, p_z-wave pairing, and $(p_z + {\rm i}p_y)$-wave pairing are plotted in panels (a), (b), and (c), respectively. The values of the angle $a_{\rm R}$ are shown in the figures. The other parameters are $\Delta/\mu_{\rm s} = 0.001$, $\alpha = 0.1$, $V_x = 0.1$, $T/T_{\rm c} = 0.4$, $k_{\rm F}L = 20$, $a_{\rm L} = 0$.

4. Conclusion

In summary, we have theoretically studied the influence of Rashba SOI on Josephson effect in junctions consisting of two spin-triplet p-wave superconductors connected by a 2D semiconductor channel with strong Rashba SOI. The variations of the supercurrent and current-phase relation with the relevant physical parameters are investigated in some detail. It is found that the magnitude of the supercurrent exhibits significant oscillations with the Rashba SOI strength, but the amplitude of the oscillation decreases gradually with the increase of the Rashba SOI strength. Accompanying with the oscillations of the magnitude of the supercurrent, 0–π transitions may also be driven by varying the Rashba SOI strength. It is also shown that if both Rashba SOI and Zeeman magnetic field are present, the significant oscillation of the supercurrent with the Rashba SOI strength or with the magnetic field strength may be suppressed substantially or may even be smeared out by their interplay. Furthermore, it is shown that the relative orientations of the $\boldsymbol{d}$ vectors in two superconducting leads of a junction may also play an important role in the supercurrent and the current-phase relationship, and 0–π transitions can also be realized by changing the relative orientations of the $\boldsymbol{d}$ vectors in two superconducting leads.

References

[1] Žutić I, Fabian J and Das Sarma S 2004 *Rev. Mod. Phys.* **76** 323
[2] Winkler R 2003 *Spin–Orbit Coupling Effects in Two-Dimensional Electron and Hole Systems* (Berlin: Springer)
[3] Dresselhaus G 1955 *Phys. Rev.* **100** 580
[4] Bychkov Y A and Rashba E I 1984 *J. Phys. C* **17** 6039
[5] Koralek J D, Weber C P, Orenstein J, Bernevig B A, Zhang S C, Mack S and Awschalom D D 2009 *Nature* **458** 610
[6] Fu J, Penteado P H, Hachiya M O, Loss D and Egues J C 2016 *Phys. Rev. Lett.* **117** 226401
[7] Marinescu D C, Weigele P J, Zumbuhl D M and Egues J C 2019 *Phys. Rev. Lett.* **122** 156601
[8] Kato Y K, Myers R C, Gossard A C and Awschalom D D 2004 *Science* **306** 1910
[9] Sih V, Myers R C, Kato Y K, Lau W H, Gossard A C and Awschalom D D 2005 *Nat. Phys.* **1** 31
[10] Stern N P, Ghosh S, Xiang G, Zhu M, Samarth N and Awschalom D D 2006 *Phys. Rev. Lett.* **97** 126603
[11] Valenzuela S O and Tinkham M 2006 *Nature* **442** 176
[12] Kane C L and Mele E J 2006 *Science* **314** 1692
[13] König M, Wiedmann S, Bruene C, Roth A, Buhmann H, Molenkamp L W, Qi X L and Zhang S C 2007 *Science* **318** 766
[14] Hasan M Z and Kane C L 2010 *Rev. Mod. Phys.* **82** 3045
[15] Qi X L and Zhang S C 2011 *Rev. Mod. Phys.* **83** 1057
[16] Franceschi S D, Kouwenhoven L, Schoenenberger C and Wernsdorfer W 2010 *Nat. Nanotechnol.* **5** 703
[17] Van Dam J A, Nazarov Y V, Bakkers E P A M, Franceschi S D and Kouwenhoven L P 2006 *Nature* **442** 667
[18] Katsaros G 2010 *Nat. Nanotechnol.* **5** 458
[19] Dirks T, Hughes T L, Lal S, Uchoa B, Chen Y F, Chialvo C, Goldbart P M and Mason N 2011 *Nat. Phys.* **7** 386
[20] Kasumov A Y, Deblock R, Kociak M, Reulet B, Bouchiat H, Khodos I I, Gorbatov Y B, Volkov V T, Journet C and Burghard M 1999 *Science* **284** 1508
[21] Morpurgo A F, Kong J, Marcus C M and Dai H 1999 *Science* **286** 263
[22] Doh Y, Van Dam J, Roest A, Bakkers E, Kouwenhoven L and Franceschi S D 2005 *Science* **309** 272
[23] Xiang J 2006 *Nat. Nanotechnol.* **1** 208
[24] Cheng M and Lutchyn R M 2012 *Phys. Rev. B* **86** 134522
[25] Yokoyama T, Eto M and Nazarov Y V 2014 *Phys. Rev. B* **89** 195407
[26] Alidoust M 2020 *Phys. Rev. B* **101** 155123
[27] Beenakker C W J, Pikulin D I, Hyart T, Schomerus H and Dahlhaus J P 2003 *Phys. Rev. Lett.* **110** 017003
[28] Buzdin A 2008 *Phys. Rev. Lett.* **101** 107005
[29] Reynoso A A, Usaj G, Balseiro C A, Feinberg D and Avignon M 2008 *Phys. Rev. Lett.* **101** 107001
[30] Liu J F and Chan K S 2010 *Phys. Rev. B* **82** 125305
[31] Zazunov A, Egger R, Jonckheere T and Martin T 2009 *Phys. Rev. Lett.* **103** 147004
[32] Costa A and Fabian J 2020 *Phys. Rev. B* **101** 104508
[33] Maeno Y, Hashimoto H, Yoshida K, Nishizaki S, Fujita T, Bednorz J G and Lichtenberg F 1994 *Nature* **372** 532
[34] Mathur N D, Grosche F M, Julian S R, Walker I R, Freye D M, Haselwimmer R K W and Lonzarich G G 1998 *Nature* **394** 39
[35] Fukumoto T, Taguchi K, Kobayashi S and Tanaka Y 2015 *Phys. Rev. B* **92** 144514
[36] Hu C R 1994 *Phys. Rev. Lett.* **72** 1526
[37] Furusaki A and Tsukada M 1991 *Solid State Commun.* **78** 299
[38] Kashiwaya S and Tanaka Y 2000 *Rep. Prog. Phys.* **63** 1641
[39] Asano Y 2006 *Phys. Rev. B* **72** 092508
[40] Asano Y 2006 *Phys. Rev. B* **74** 220501